Asian Journal of Chemistry; Vol. 31, No. 3 (2019), 559-565

ASIAN JOURNAL OF CHEMISTRY

https://doi.org/10.14233/ajchem.2019.21682

Enhanced Solar Water Splitting Performance of 50-100 nm Pore Sized TiO_2 Nanotubes

K. KATHIRESAN[1], P. ELANGOVAN[2,*] and M.S.S. SARAVANAKUMAAR[3]

[1]Department of Physics, P.S.N.A. College of Engineering & Technology, Dindigul-624622, India
[2]PG & Research Department of Physics, Pachaiyappa's College, Chennai-600030, India
[3]Department of Physics, Saraswathi Narayanan College (Autonomous), Madurai-625022, India

*Corresponding author: E-mail: drelangovanphysics@gmail.com

Received: 29 August 2018; *Accepted*: 22 October 2018; *Published online*: 31 January 2019; AJC-19245

Herein, we report the fabrication of titanium dioxide nanotubes *via* anodization technique through with and without hydrofluoric acid . The impact of hydrofluoric acid followed by annealing effect on TiO_2 nanotubes for the solar water splitting performance was examined. Prepared TiO_2 samples exhibited a diameter of about 50 to 100 nm sized nanotubes and hierarchical structures and they subjected to annealing. Synthesis and annealing effects on chemical, physical and photoelectrochemical water splitting activity of TiO_2 samples were scrutinized. The crystalline nature, structure and surface morphologies of prepared TiO_2 photocatalysts were explored by X-ray diffraction, scanning electron microscope, and the oxidation states of both titanium and oxygen was determined by X-ray photoelectron spectroscopy. As a consequence, after annealing at 500 ºC, TiO_2 thin films treated with hydrofluoric acid solution (HF-TiO_2) were found to exhibit a remarkable photoelectrochemical performance than bare TiO_2 nanotubes under UV light irradiation. Moreover, the mechanistic insights acquired in the current research would be beneficial to design a novel and highly efficient photocatalyst for solar water splitting systems.

Keywords: TiO_2 nanotubes, Hydrofluoric acid, Water splitting, Band blending, Hydrogen energy.

INTRODUCTION

Recent era, an interface of semiconductor-liquids signifies an inspiring and important part, involving principles of several research areas including, electrocatalysts and photocatalysts, *etc*. Most of them are dedicated on renewable energy conversion systems, over the use of solar water splitting cells (*i.e*. photoelectrochemical cells), which convert photons (light) to electricity [1,2]. Likely, an important application involves the improvement of photocatalytic procedures for selective photo-oxidation as well as for environmental remediation of harmful organic compounds. Typically, during photocatalytic reactions, the incident light of photons used to trigger a photocatalytic substance (*i.e*. photocatalyst) and which could stimulate the rate of a chemical reactions. Photoelectrochemical (PEC) water splitting is enormously good-looking for an extent reasons [3,4] including, (i) non-polluting and environment friendly (ii) photogenerated hydrogen is a valuable fuel and it is a revered chemical used by chemical industries to produce ammonia and petroleum purifying and (iii) cost effective. Significantly, the choice of an ideal PEC photoanode material is crucial, since their band gaps regulates its photo-response to the complete solar spectrum particularly visible light spectrum. Besides, which could permit the splitting of water process with a lowest applied bias voltage [5]. Almost nearly half century, many researchers have tried to identify suitable semiconductors for water splitting [6-14].

In this respect, studies have dedicated on oxides and more recently, on oxynitrides, organic and inorganic nanocomposites due to their good functional properties with respect to stability [15-21]. Among them, water-splitting using TiO_2 both in rutile (energy gap = 3eV) and anatase phases (energy gap = 3.2eV) for water splitting deals a favourable approach for a clean, inexpensive and eco-friendly generation of hydrogen by solar energy [22,23]. Since the discovery of photoelectrochemical water splitting using TiO_2 electrodes was approved to harvest hydrogen and/or oxygen (O_2) from aqueous electrolytic solutions. It has been proven that TiO_2 photoelectrodes with nanostructures revealed a higher photochemical performance than their bulk form, this decreased performance of bulk TiO_2 was

mainly due to the short diffusion lengths [24]. In specific, the arrays of TiO_2 nanotubes displays a facile and oriented charge transport functionalities, which leads to an enlarged scattering of free electrons and decreases the mobility of electrons [25,26]. However, for TiO_2 nanotube photo-anodes, the practically reported photo-conversion efficiencies are lower than the theoretical limits. Thus, recent years, several kinds of TiO_2 photo-anodes with nanotubes of ~ 0.5-1000 μm [27,28] length and pore size of ~ 12-350 nm [29,30] wall thickness ~ 5-40 nm [31] and tube-to-tube design with a few tens of nanometers have been testified [32]. Initially, TiO_2 nanotubes of 400-500 nm in length, were fabricated with anodization of Ti for aqueous solution containing F^- by Grimes and Mor [33]. Later, up to 1 mm in length, was produced using polar solution such as formaldehyde, ethylene glycol, dimethyl sulfoxide containing fluoride. It was evidently clear that there is no need to include F^- in the solution for fabricating TiO_2. It was possible to produce the nanotubes using HCl and H_2O_2 solution. Initially, an advanced TiO_2 nanotubes were manufactured by Grimes *et al.* [34] with the use of electrolyte of hydrofluoric acid through anodization [34]. Later, several research investigations were advanced to regulate and/or modify the nanotubes structures such as morphology, length and pore size, and the wall thickness [35]. Till now, numerous studies had been done for hydrogen production using TiO_2 nanotube arrays and the outcomes revealed outstanding response to incoming light photons [36,37].

It is well known that by high temperature annealing effect, the electrical, optical, structural and functional properties of various nanostructures can be modified in high degree [38]. In this aspect, herein, TiO_2 nanotubes (TNT′s) were fabricated *via* a simple anodization method. The effect of temperature on the TiO_2 nanotubes, the crystal structure, chemical composition, surface morphology and photo-response characteristic of TiO_2 nanotubes films was studied in detail. This work demonstrates that a high temperature of 500 ºC can be used to modify the surface structure of photocatalysts to significantly improve photocatalytic performance for hydrofluoric acid influenced TiO_2 nanotubes at ~ 50-100 nm pore size. The effect of hydrofluoric acid loading content and the temperature effect on TiO_2 nanotubes on the rates of photocatalytic hydrogen production of prepared samples in KOH solution was investigated.

EXPERIMENTAL

Initially, pure titanium foil (thickness ~ 0.25 mm and purity ~ 99.7 %) was obtained from Alfa Aesar. The foil was cleaned by sonication in a solution of acetone/methanol for 30 min. Nanotubes of titania prepared by anodizing titanium foil in electrolyte solution (0.5 % hydrofluoric acid). Anode contains Ti metal foil in the electrochemical system, where platinum was used as a cathode. About 5 mL of HF electrolyte solution was used for each anodization method, and 2.1 cm^2 of titanium foil surface was exposed (*i.e.* immersed) to the electrolyte. A constant potential of ~ 25 V was applied about ~ 30 min to run the anodization process. Finally, the samples were then annealed at 500 ºC in a furnace (heating rate: 25 ºC/min) for 5 h. Alongside, H_2O_2 was used to prepare TiO_2 hierarchical structure. For easy identification, as prepared hierarchical TiO_2 was named as TH-AP; and its annealed sample was TH-500. Likely, the TiO_2 nanotube samples were denoted as TT-AP for as prepared sample and TT-500 for annealed samples.

The prepared TiO_2 nanotube films were characterized by means of several analytical techniques. The microstructures of TiO_2 nanotubes were scrutinized by scanning electron microscopy (SEM, XL30-SFEG Phillips Co., Holland at 10 kV). The crystalline nature of the samples were identified by X-ray diffraction (XRD, Rigaku Japan, D/MAX-2500), using CuKα radiation over a 2θ range of 20º to 80º, respectively. The chemical compositions of prepared TiO_2 nanotube samples were examined by XPS measurement (Thermo Fisher Scientific with a monochromatic Al Kα X-ray source (1486.6 eV)). Photoelectrochemical (PEC) water splitting experiment was perceived in a three-electrode set-up using a VersaSTAT-3 potentio-stat, Princeton Applied Research, USA. TiO_2 nanotubes film was used as a working electrode (exposed working electrode area of ~1 cm^2), Ag/AgCl in KCl saturated solution was used as a reference electrode and platinum wire as the counter electrode. Nitrogen saturated 5.0 M NaOH was used as electrolyte. The light source of 400 W Xenon arc lamp (AM 1.5 conditions, 100 mW cm^{-2}, Newport solar simulator) was used. The linear sweep voltammograms for photoelectrochemical (PEC) experiments were done over a scan rate of 10 mV/s.

RESULTS AND DISCUSSION

Structural and morphological studies: Fig. 1 displays the XRD patterns of bare and annealed TiO_2 photoanodes including TT-AP and TH-AP samples. From XRD results, all the TiO_2 photoanodes comprising an anatase and rutile phases, while anatase is the main component for TT-AP and TH-AP. There is slight change in intensity of XRD diffraction pattern for TT-AP, before and after annealing. This means that there is no strong phase transition occurred after the annealing. The diffraction pattern of TiO_2 nano tube at TT-AP shows the peaks of minimal intensities before the irradiation, after the irradiation the intensity of the peak at 38.10º increased tremendously at the same time the peak intensity at ~ 40 lowered down. This is the indication for structural phase transition. However, the peak intensity slightly increased during annealing. The XRD peaks at ~ 25.14º, 38.10º, 48.06º, 53.5º, 54.28º, 62.60º and 69.70º was assigned to (101), (004), (200), (105), (211), (204) and (220) anatase planes (according to the JCPDS 21-1272 diffraction pattern) while the peaks at ~ 27.4º and 35.90º are in good agreement with the (110) and (100), planes of the rutile phase (JCPDS 21-1276). Later, benefiting from annealing effect, the intensity of the diffraction peaks analogous to the anatase and rutile phases are getting increased. This was accredited to the annealing effect [39], besides, annealing is renowned to improve the crystalline nature of the material [40].

Figs. 2 and 3 show the surface morphology of prepared TH-AP, TH-500, TT-AP and TT-500 samples. This illustrative image of a nanotube array nearly hierarchical (Fig. 2) and ~ 50-100 nm in diameter nanotube arrays (Fig. 3). The TH-AP sample exhibits the denser arrays and after annealing, there are certain changes in the surface area. It is due to the temperature effect. From Fig. 3, the average diameter of these nanotubes was about ~50-100 nm, wall thickness ~15 nm. After the

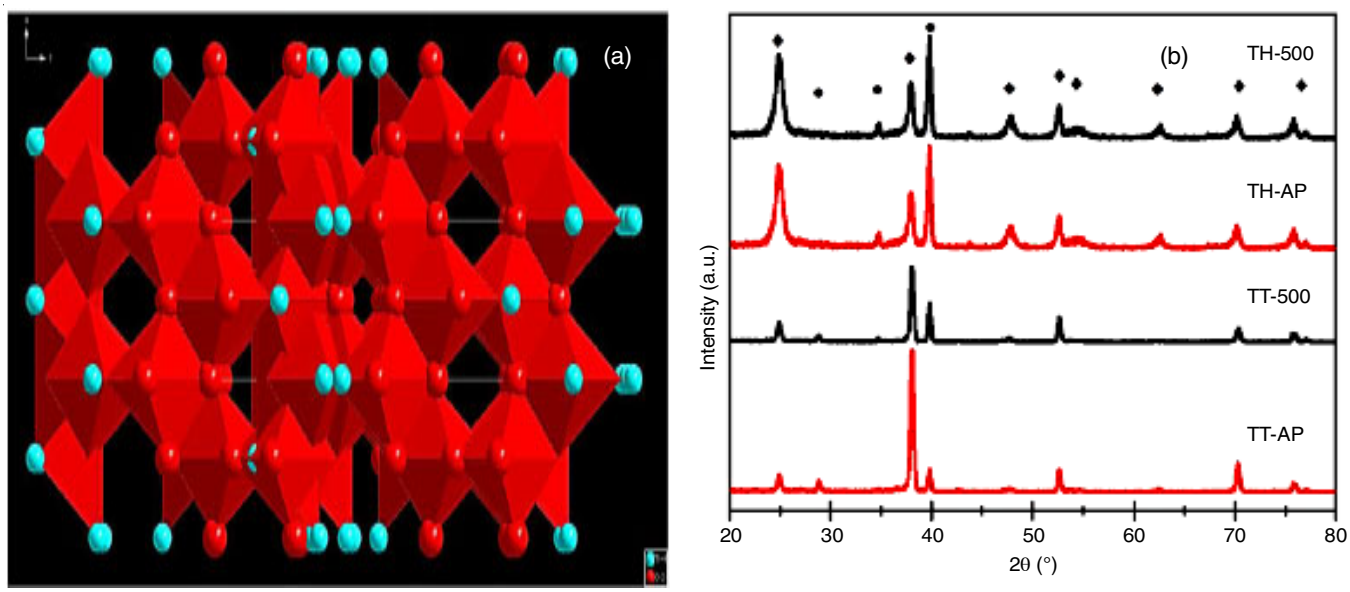

Fig. 1. (a) Structure of TiO_2 and (b) XRD pattern of pristine and annealed TiO_2 hierarchical and nanotubes samples

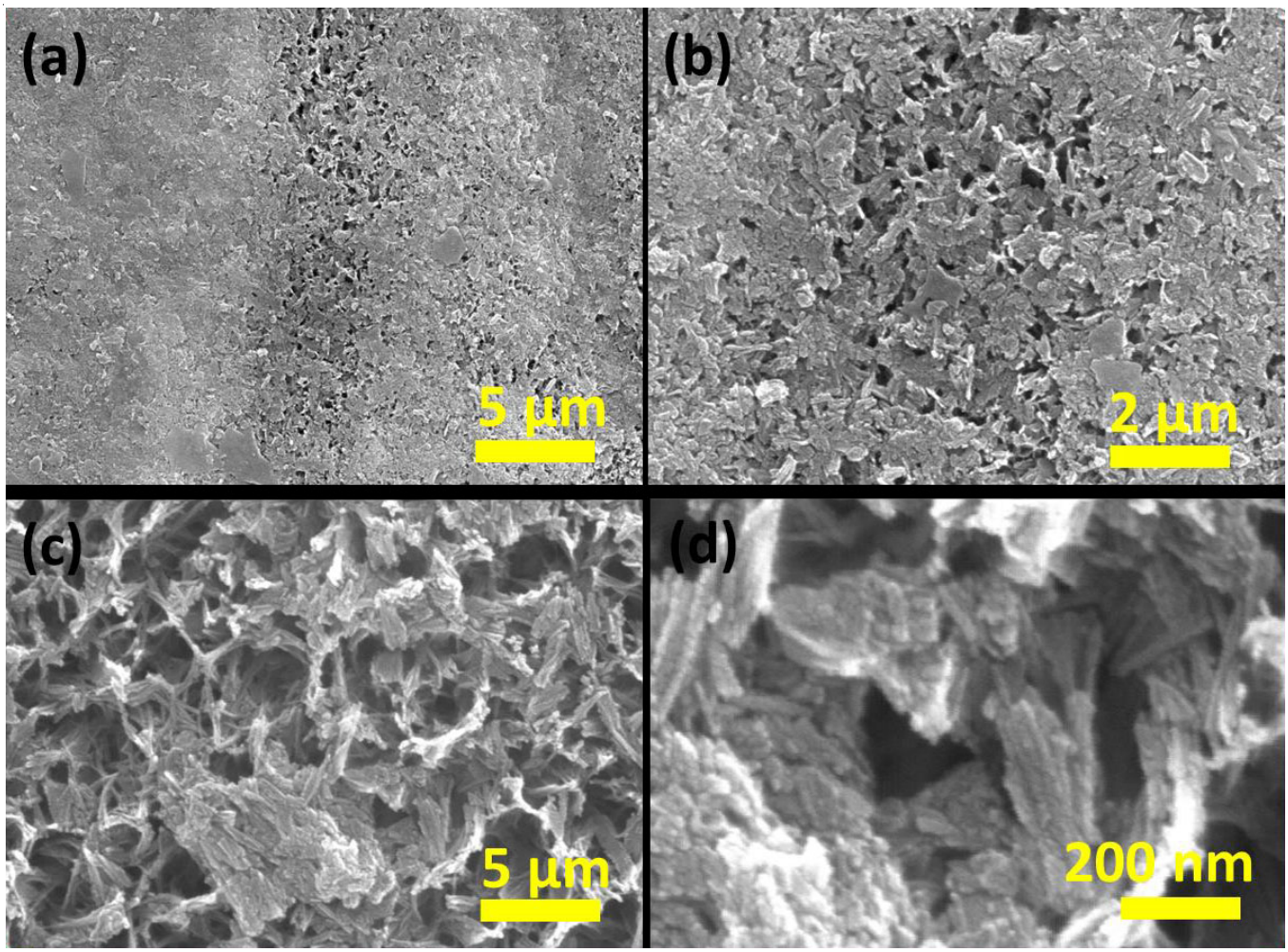

Fig. 2. SEM images of (a-b) for TH-AP and (c-d) for TH 500 samples

annealing, the sample exhibits a surface change. However, the temperature effect on HF-TiO_2 nanotubes improves the quality of the nanotubes with the addition of HF. For HF-TiO_2 after annealing, the well-aligned regular porous in TiO_2 structure consisted of nano pore arrays with an even pore diameter. Nanotube arrays were obtained in a 0.5 wt. % HF solution. $TiO_2 + 6F^- + 4H^+ \rightarrow TiF_6^{2-} + 2H_2O$. Further, by this reaction conditions, the higher field at the bottom of pores could able to promote the oxidation of titanium [41]. Besides, the metallic region among the pores might also endure a related alteration leading

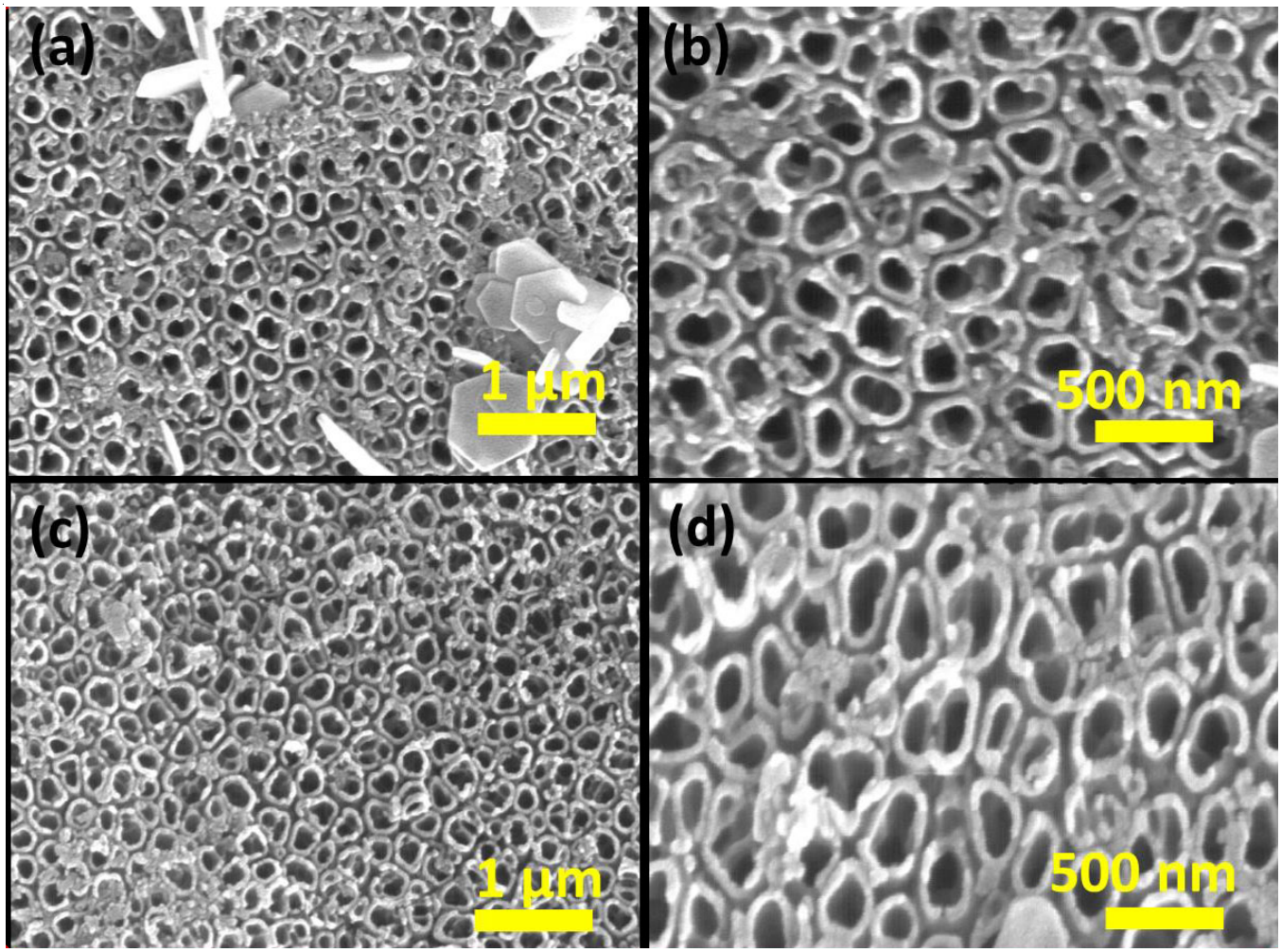

Fig. 3. SEM images of (a-b) for TT-AP and (c-d) for TT 500 samples

to tube structure development. Remarkably, the chemical dissolution of the oxide at the pore mouth by F^- influences the particular degree of pore creation. In addition, H^+ ion concentration was reduced by the water content in HF/water electrolyte, which controls the dissolution reaction. Also, the volume of water ensures the field supported etching of Ti foil at the bottom of the pores [42,43].

X-ray photoelectron analysis: X-ray photoelectron spectroscopic measurement (XPS) was used to study the chemical composition of TiO_2 nanotubes interfaces. Fig. 4 represents the overall XPS spectra for all the prepared samples. Notably, after annealing, the core-level of Ti 2p state (Fig. 5a) of TiO_2 nanotubes obviously presenting a peak shift towards a higher binding energy. This energy shift might be owed to the band discontinuity effect (band bending). Such core-level binding energy shift was attributed to changes in coordination of metal oxide and has been renowned in several metal oxide systems [44-46]. This validates the effect of temperature on the surface of TiO_2, whereas annealed at 500 ºC. Moreover, the lower binding energies broadening was owing to the surface reduction of Ti^{4+} species to intermediate oxidation states [47,48]. This results are in good agreement with previously reported results [49]. Fig. 5b showing the O1s core-level spectra of prepared samples, whereas, the peak broadening were accredited to a loss of the long-range order in TiO_2 (before annealing-black line spectra),

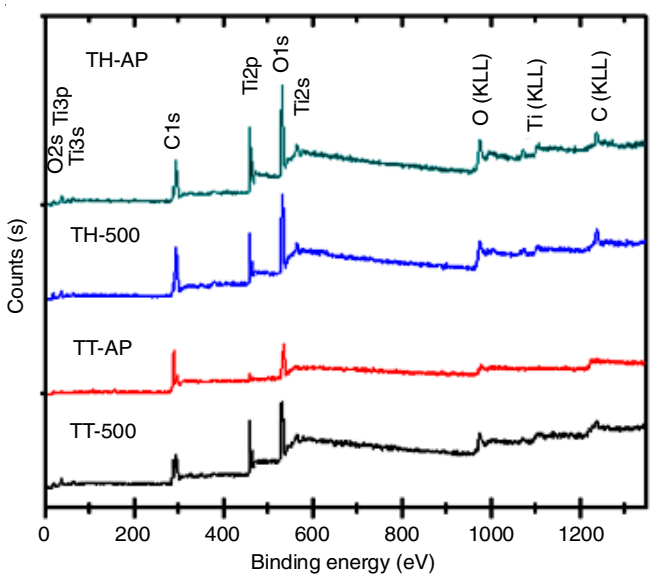

Fig. 4. XPS spectra of TiO_2 samples

it was mainly originates from the interactions of titanium with second-neighbour atoms. Moreover, after annealing, the TiO_2 samples exhibited some extent of narrow peaks (after annealing -red line spectra). This is evidently revealing that after the anneaaling, the crystalline natures of TiO_2 nanotubes were greatly

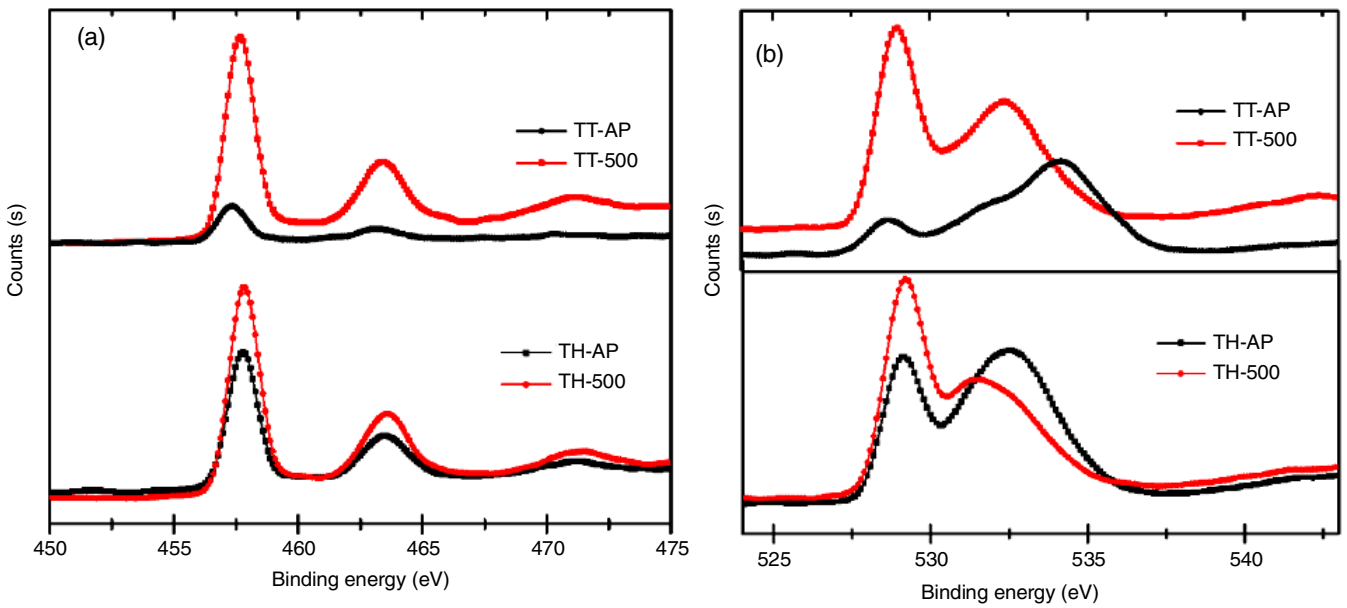

Fig. 5. XPS spectra of (a) Ti2p and (b) O1s levels of TiO_2 samples

enhanced. Table-1 displays the summarized XPS peak values of TiO_2 samples. Likely, the intensity of XPS peaks dissimilar with the density of vacant *d*-states, which is dependable with an increasing amount of Ti^{4+} cations. Hence, annealing effect could lead to improve the oxidation of Ti cations and to form well-ordered TiO_2 [49,50].

Photoelectrochemical (PEC) study: Fig. 6 represents the linear sweep voltammograms (LSV) of TiO_2 nanotube photoelectrodes, whereas, photocurrent density (J) *vs*. potential (V) was measured in 5 M KOH electrolyte solution. As shown in Fig. 6, the photocurrent density (J) was plotted against applied potential (V), at higher anodic polarization, the J-V plot deviates from linearity for all the samples, this was mainly due to band bending effect of prepared photoanodes [51]. Under dark condition, there is no noticeable photocurrent was perceived. However, under UV light condition, all the photoanodes exhibited an enhanced photocurrent. Particularly, at -0.45 V to 1.2 V *vs*. Ag/AgCl, the photocurrent density of TT-500 photoanode

TABLE-1
CORRESPONDING XPS PEAK VALUES PREPARED SAMPLES

Samples	O1s	$Ti2p_{1/2}$	$Ti2p_{3/2}$	Ti3s	O2s	Ti3p	C1s
TT-500	529.4	463.8	458.15	60.89	20.98	36.58	285.70
TT-AP	528.5	463.5	458.10	60.40	21.05	36.81	285.18
TH-AP	529.5	463.5	457.94	60.57	20.92	36.40	285.09
TH-500	529.0	463.8	457.50	60.75	21.03	36.87	284.90

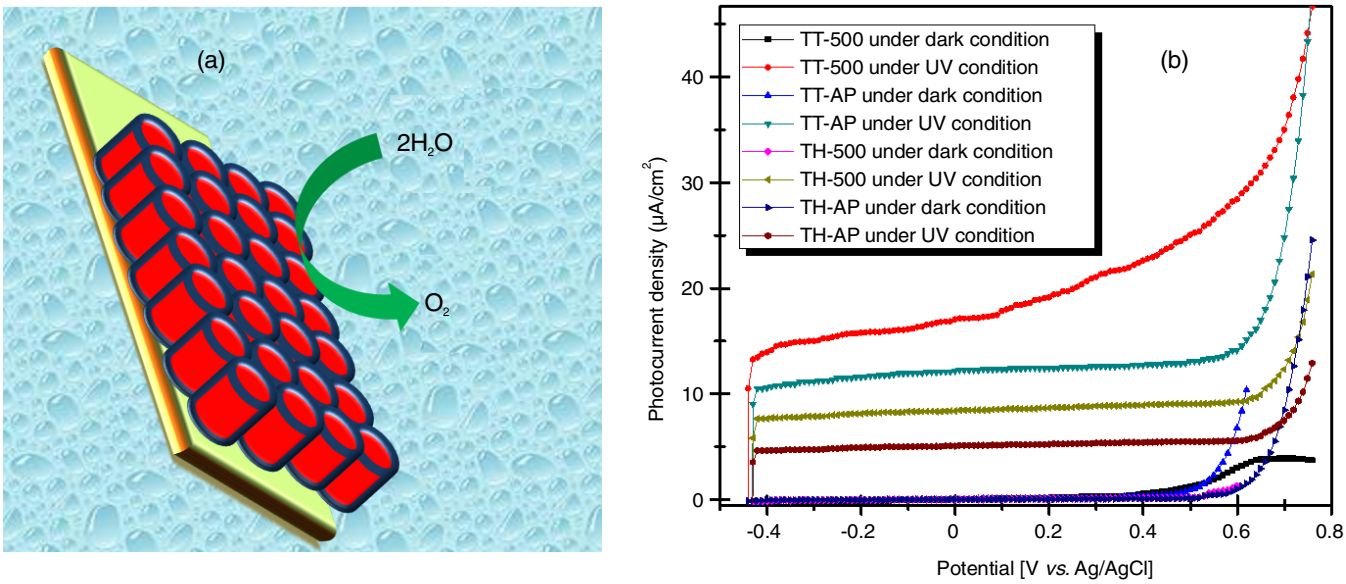

Fig. 6. (a) Schematic diagram and (b) the corresponding PEC water splitting performance of TiO_2 hierarchical structure and nanotubes

was higher than all other samples. Significantly, the TT-500 photoanode surveyed linearity over the high bias voltage ranges. Typically, as-prepared samples of TH-AP and TT-AP (*i.e.* before annealing) exhibited a low photocurrent density than annealed photoanodes (*i.e.* TH-500 and TT-500). The enhanced performance of TT-500 photoanode was mainly attributed to the large active surface area, crystalline nature and denser nanotube arrays [52]. Similarly, Lagemaat *et al.* [53] revealed a considerable PEC improvement of SiC prepared by anodic etching using HF solution. Typically, the nanometer systems hold small sized particles; they ensure their capacity to sustain a significant amount of band bending. Also, the enriched band bending of the thicker walls reduces the surface recombination of photogenerated charges, thus the photocurrent is getting increased. Predominantly, TiO_2 nanotubes fabricated using HF electrolyte was exhibited longer diameter than those without HF. The variation in diameter is extremely sufficient to positively influence the photo-response of nanotube photoelectrodes. At the same time, the PEC performance of HF/TiO_2 at 50-100 nm electrode was further enhanced by annealing effect. The photogenerated electrons and holes in these HF-treated TiO_2 followed by annealing might, thus, are consumed more efficiently as compared with untreated TiO_2 due to the prolonged contact area among the photocatalyst and electrolyte.

Conclusion

In this work, the photo-response characteristics of TiO_2 nanotubes are discussed by the effect of band blending. It is observed that the photo-response activity is enhanced by both HF and annealing effect. From the XPS and photoelectrochemical studies, it strongly suggests impact of band blending of TiO_2 nanotubes on PEC water splitting. The changes in crystal structure, chemical composition and morphology of TiO_2 films were greatly affected and remarkably improved by high temperature annealing effect.

CONFLICT OF INTEREST

The authors declare that there is no conflict of interests regarding the publication of this article.

REFERENCES

1. A. Fujishima and K. Honda, *Nature*, **238**, 37 (1972); https://doi.org/10.1038/238037a0.
2. K. Rajeshwar, *J. Appl. Electrochem.*, **37**, 765 (2007); https://doi.org/10.1007/s10800-007-9333-1.
3. S. Caramori, V. Cristino, R. Argazzi, L. Meda and C.A. Bignozzi, *Inorg. Chem.*, **49**, 3320 (2010); https://doi.org/10.1021/ic9023037.
4. A.J. Nozik and R. Memming, *J. Phys. Chem.*, **100**, 13061 (1996); https://doi.org/10.1021/jp953720e.
5. M. Ni, M.K.H. Leung, D.Y.C. Leung and K. Sumathy, *Renew. Sustain. Energy Rev.*, **11**, 401 (2007); https://doi.org/10.1016/j.rser.2005.01.009.
6. K.-S. Ahn, Y. Yan, S. Shet, K. Jones, T. Deutsch, J. Turner and M. Al-Jassim, *Appl. Phys. Lett.*, **93**, 163117 (2008); https://doi.org/10.1063/1.3002282.
7. V. Chakrapani, J. Thangala and M.K. Sunkara, *Int. J. Hydrogen Energy*, **34**, 9050 (2009); https://doi.org/10.1016/j.ijhydene.2009.09.031.
8. B.D. Alexander, P.J. Kulesza, I. Rutkowska, R. Solarska and J. Augustynski, *J. Mater. Chem.*, **18**, 2298 (2008); https://doi.org/10.1039/b718644d.
9. J. Su, L. Guo, S. Yoriya and C.A. Grimes, *Cryst. Growth Des.*, **10**, 856 (2010); https://doi.org/10.1021/cg9012125.
10. A. Duret and M. Grätzel, *J. Phys. Chem. B*, **109**, 17184 (2005); https://doi.org/10.1021/jp044127c.
11. S.K. Mohapatra, S.E. John, S. Banerjee and M. Misra, *Chem. Mater.*, **21**, 3048 (2009); https://doi.org/10.1021/cm8030208.
12. J. Brillet, M. Gratzel and K. Sivula, *Nano Lett.*, **10**, 4155 (2010); https://doi.org/10.1021/nl102708c.
13. R. Morrish, M. Rahman, J. MacElroy and C.A. Wolden, *ChemSusChem*, **4**, 474 (2011); https://doi.org/10.1002/cssc.201100066.
14. H.M. Chen, C.K. Chen, R.-S. Liu, L. Zhang, J. Zhang and D.P. Wilkinson, *Chem. Soc. Rev.*, **41**, 5654 (2012); https://doi.org/10.1039/c2cs35019j.
15. F.E. Osterloh, *Chem. Mater.*, **20**, 35 (2008); https://doi.org/10.1021/cm7024203.
16. S. Chandrasekaran, C. Bowen, P. Zhang, Z. Li, Q. Yuan, X. Ren and L. Deng, *J. Mater. Chem. A Mater. Energy Sustain.*, **6**, 11078 (2018); https://doi.org/10.1039/C8TA03669A.
17. S. Chandrasekaran, E.J. Kim, J.S. Chung, I.-K. Yoo, V. Senthilkumar, Y.S. Kim, C.R. Bowen, V. Adamaki and S. Hyun Hur, *Chem. Eng. J.*, **309**, 682 (2017); https://doi.org/10.1016/j.cej.2016.10.087.
18. S. Chandrasekaran, Y.-L.T. Ngo, L. Sui, E.J. Kim, D.K. Dang, J.S. Chung and S.H. Hur, *Dalton Trans.*, **46**, 13912 (2017); https://doi.org/10.1039/C7DT02936E.
19. S. Chandrasekaran, J.S. Chung, E.J. Kim and S.H. Hur, *Chem. Eng. J.*, **290**, 465 (2016); https://doi.org/10.1016/j.cej.2016.01.029.
20. S. Chandrasekaran, E.J. Kim, J.S. Chung, C.R. Bowen, B. Rajagopalan, V. Adamaki, R.D.K. Misra and S.H. Hur, *J. Mater. Chem. A Mater. Energy Sustain.*, **4**, 13271 (2016); https://doi.org/10.1039/C6TA05043C.
21. S. Chandrasekaran, S.H. Hur, W.M. Choi, J.S. Chung and E.J. Kim, *Mater. Lett.*, **160**, 92 (2015); https://doi.org/10.1016/j.matlet.2015.07.091.
22. A. Galinska and J. Walendziewski, *Energy Fuels*, **19**, 1143 (2005); https://doi.org/10.1021/ef0400619.
23. J. Tang, J.R. Durrant and D.R. Klug, *J. Am. Chem. Soc.*, **130**, 13885 (2008); https://doi.org/10.1021/ja8034637.
24. S. Liang, J. He, Z. Sun, Q. Liu, Y. Jiang, H. Cheng, B. He, Z. Xie and S. Wei, *J. Phys. Chem. C*, **116**, 9049 (2012); https://doi.org/10.1021/jp300552s.
25. K. Shankar, J.I. Basham, N.K. Allam, O.K. Varghese, G.K. Mor, X. Feng, M. Paulose, J.A. Seabold, K.-S. Choi and C.A. Grimes, *J. Phys. Chem. C*, **113**, 6327 (2009); https://doi.org/10.1021/jp809385x.
26. W. Yan, Z. Sun, T. Yao, Z. Pan, Z. Li, Q. Liu and S. Wei, *J. Appl. Phys.*, **106**, 123918 (2009); https://doi.org/10.1063/1.3272855.
27. D. Gong, C. Grimes, O.K. Varghese, W. Hu, R. Singh, Z. Chen and E.C. Dickey, *J. Mater. Res.*, **16**, 3331 (2001); https://doi.org/10.1557/JMR.2001.0457.
28. M. Paulose, H.E. Prakasam, O.K. Varghese, L. Peng, K.C. Popat, G.K. Mor, T.A. Desai and C.A. Grimes, *J. Phys. Chem. C*, **111**, 14992 (2007); https://doi.org/10.1021/jp075258r.
29. S. Yoriya and C.A. Grimes, *Langmuir*, **26**, 417 (2010); https://doi.org/10.1021/la9020146.
30. K. Shankar, G.K. Mor, A. Fitzgerald and C.A. Grimes, *J. Phys. Chem. C*, **111**, 21 (2007); https://doi.org/10.1021/jp066352v.
31. C. Ruan, M. Paulose, O.K. Varghese, G.K. Mor and C.A. Grimes, *J. Phys. Chem. B*, **109**, 15754 (2005); https://doi.org/10.1021/jp052736u.
32. S. Yoriya and C.A. Grimes, *J. Mater. Chem.*, **21**, 102 (2011); https://doi.org/10.1039/C0JM02421J.
33. C.A. Grimes and G.K. Mor, TiO_2 Nanotube Arrays: Synthesis, Properties and Applications, Springer, 2009.
34. G.K. Mor, O.K. Varghese, M. Paulose, K. Shankar and C.A. Grimes, *Sol. Energy Mater. Sol. Cells*, **90**, 2011 (2006); https://doi.org/10.1016/j.solmat.2006.04.007.

35. J. Macak, H. Tsuchiya, A. Ghicov, K. Yasuda, R. Hahn, S. Bauer and P. Schmuki, *Curr. Opin. Solid State Mater. Sci.*, **11**, 3 (2007); https://doi.org/10.1016/j.cossms.2007.08.004.
36. O.K. Varghese, D. Gong, M. Paulose, K.G. Ong and C.A. Grimes, *Sens. Actuators B Chem.*, **93**, 338 (2003); https://doi.org/10.1016/S0925-4005(03)00222-3.
37. E. Sennik, Z. Çolak, N. Kilinç and Z.Z. Öztürk, *Int. J. Hydrogen Energy*, **35**, 4420 (2010); https://doi.org/10.1016/j.ijhydene.2010.01.100.
38. C.P. Puls, N.E. Staley, J.-S. Moon, J.A. Robinson, P.M. Campbell, J.L. Tedesco, R.L. Myers-Ward, C.R. Eddy Jr., D.K. Gaskill and Y. Liu, *Appl. Phys. Lett.*, **99**, 013103 (2011); https://doi.org/10.1063/1.3607284.
39. P. Romero-Gomez, A. Palmero, T. Ben, J. Lozano, S. Molina and A. González-Elipe, *Phys. Rev. B*, **82**, 115420 (2010); https://doi.org/10.1103/PhysRevB.82.115420.
40. D.S. Dhawale, D.P. Dubal, R.R. Salunkhe, T.P. Gujar, M.C. Rath and C.D. Lokhande, *J. Alloys Compd.*, **499**, 63 (2010); https://doi.org/10.1016/j.jallcom.2010.01.126.
41. B. Chen, J. Hou and K. Lu, *Langmuir*, **29**, 5911 (2013); https://doi.org/10.1021/la400586r.
42. J.M. Macak, H. Hildebrand, U. Marten-Jahns and P. Schmuki, *J. Electroanal. Chem.*, **621**, 254 (2008); https://doi.org/10.1016/j.jelechem.2008.01.005.
43. A. Ghicov and P. Schmuki, *Chem. Commun.*, 2791 (2009); https://doi.org/10.1039/b822726h.
44. B.M. Reddy, B. Chowdhury and P.G. Smirniotis, *Appl. Catal. A Gen.*, **211**, 19 (2001); https://doi.org/10.1016/S0926-860X(00)00834-6.
45. R. Reiche, S. Oswald, F. Yubero, J.P. Espinos, J.P. Holgado and A.R. Gonzalez-Elipe, *J. Phys. Chem. B*, **108**, 9905 (2004); https://doi.org/10.1021/jp031274m.
46. S. Chandrasekaran, *Sol. Energy Mater. Sol. Cells*, **109**, 220 (2013); https://doi.org/10.1016/j.solmat.2012.11.003.
47. G. Silversmit, G. De Doncker and R. De Gryse, *Surf. Sci. Spectra*, **9**, 21 (2002); https://doi.org/10.1116/11.20020701.
48. M.-Y. Hsu, W.-C. Yang, H. Teng and J. Leu, *J. Electrochem. Soc.*, **158**, K81 (2011); https://doi.org/10.1149/1.3533388.
49. J. Mayer, U. Diebold, T. Madey and E. Garfunkel, *J. Electron Spectrosc. Relat. Phenom.*, **73**, 1 (1995); https://doi.org/10.1016/0368-2048(94)02258-5.
50. U. Diebold and T. Madey, *Surf. Sci. Spectra*, **4**, 227 (1996); https://doi.org/10.1116/1.1247794.
51. Y.V. Pleskov and M. Krotova, *Electrochim. Acta*, **38**, 107 (1993); https://doi.org/10.1016/0013-4686(93)80015-R.
52. J.P. Sukamto, C.S. McMillan and W. Smyrl, *Electrochim. Acta*, **38**, 15 (1993); https://doi.org/10.1016/0013-4686(93)80005-K.
53. J. Van de Lagemaat, M. Plakman, D. Vanmaekelbergh and J. Kelly, *Appl. Phys. Lett.*, **69**, 2246 (1996); https://doi.org/10.1063/1.117142.